Hindawi
Journal of Sensors
Volume 2018, Article ID 7801597, 7 pages
https://doi.org/10.1155/2018/7801597

Research Article

Optimization of Electrostatic Force System Based on Newton Interpolation Method

Yelong Zheng,[1] Meirong Zhao,[1] Peiyuan Sun,[1] and Le Song[2]

[1]*State Key Laboratory of Precision Measuring Technology and Instruments, Tianjin University, Tianjin 300072, China*
[2]*Center of MicroNano Manufacturing Technology, Tianjin University, Tianjin 300072, China*

Correspondence should be addressed to Le Song; songle@tju.edu.cn

Received 27 June 2018; Revised 19 August 2018; Accepted 5 September 2018; Published 8 October 2018

Academic Editor: Jesus Corres

The measurements of micro/nanoforces are of great importance in both science and engineering. We developed a traceable system for micro/nanoforces based on electrostatic force using two electrodes. Noises (creep, ground vibration, and airflow) are one of the limitations for force resolution. The forces are distorted by noise and cannot be measured accurately. Although ABA method can be used to eliminate linear creep, it is invalid for nonlinear noise. In this paper, a new method known as the Newton interpolation method (NIM) has been adopted in capacitance gradient and the calibration of cantilever stiffness to reduce the effect of nonlinear noise. The results show that the capacitance gradient, with a relative standard deviation of 0.004%, is stable and has good repeatability. The stiffness of cantilever was measured using electrostatic force. The typical value of stiffness ranged from 5.1 to 48 N/m. The relative standard deviation was small, i.e., less than 0.6% owing to Newton interpolation method. These results show that our system is very stable and repeatable. This research may assist in the designing of force measurement systems based on electrostatic force.

1. Introduction

The measurement of micro/nanoforces is of great importance in both science and engineering [1–15]. It is useful in the fields of precision instruments, biology [16, 17], magnetic field distributions [18], distance measurement [19], and tribological properties of materials [20–23]. Atomic force microscope (AFM) is one of most popular microforce measurement instrument. Being the key component of AFM, the cantilever must be calibrated to measure microforces accurately. A considerable number of researches have been done on the calibration of cantilevers. The National Institute of Standards and Technology (NIST) in the USA [2], the National Physical Laboratory (NPL) in the United Kingdom [3], the Center for Measurement Standards (CMS) in Taiwan [7, 8], and the Physikalisch-Technische Bundesanstalt (PTB) in Germany [4] have all developed traceable systems that could be used for the calibration of cantilevers.

In this study, the stiffness of AFM cantilever is calibrated by an electrostatic system [2, 9] using the force-displacement curve. In general, for microforce measurements, the signal would be drowned in noise and cannot be measured accurately. The traditional force measurement systems, such as resistance strain gauge and piezo electric sensor, are vulnerable to environmental disturbances. Although linear noise may be reduced by the ABA method, higher order noise cannot be reduced. To reduce vibrations, the system at NIST was built 12 m underground. At the PTB in Germany, the nano-Newton force metrology group designed an aluminium plate pendulum; however, the resolution of the setup was constrained by noise. In order to reduce this noise, PTB set up two identical systems. This setup has a resolution of 10^{-12} N and can measure forces less than 10^{-5} N [6]. In this paper, the Newton interpolation method (NIM) is proposed to reduce the effect of noise in both the capacitance gradient determination and cantilever calibration.

2. The Electrostatic Force System

A pair of coaxial cylindrical capacitors are used to generate the electrostatic force, as shown in Figure 1. The system is placed at the centre of a 1200 mm × 900 mm optical isolation

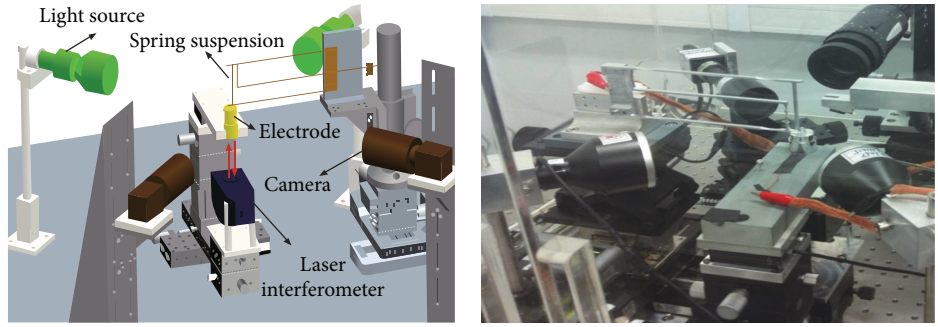

(a) (b)

Figure 1: Electrostatic force generation in the laboratory.

platform with a natural vibration of 1 Hz. The system is covered by a transparent box to reduce airflow. The experimental setup of the system is located in the China Metrology Institute Small Force Measurement Laboratory 4 m underground. The inner electrode is fixed at the end of a spring, and it moves freely along the vertical direction. The outer electrode is fixed on the frame. The electrostatic force F_e is proportional to the square of the applied voltage across the capacitor [2], as shown in (1):

$$F_e = \frac{1}{2} U^2 \frac{dC}{dz}, \tag{1}$$

where U is the voltage applied across the inner and outer electrodes, F_e is the generated electrostatic force and dC/dz is the capacitance gradient, as shown in (2):

$$\frac{dC}{dz} = \frac{2\pi\varepsilon}{\ln(R_2/R_1)}, \tag{2}$$

where R_1 is the radius of the inner electrode, R_2 is the radius of the outer electrode, and ε is the absolute permittivity.

The capacitance gradient must be determined ahead of force measurement. The capacitance gradient dC/dz is linearly proportional to the electrostatic force; the uncertainty of dC/dz will affect the force directly. To measure dC/dz accurately, the coaxial alignment of capacitor and ultraprecision machining were adopted.

A deviation from the coaxial alignment of the inner and outer electrodes results in a deviation from the ideal capacitance gradient value. A CCD camera with a pixel resolution of 2448×2050 and high-intensity backlight source was used to check the coaxial aligning status of the two cylinders. Using this setup, deviations in eccentricity and tilting of the electrode can be detected up to values of $b = 3$ μm and $\delta = 0.3^\circ$. Therefore, the maximum relative deviations in the capacitance gradient caused by eccentricity and tilt error are 0.0018% and 0.01%, respectively.

Although uncertainty in the capacitance gradient measurement is not a key factor for determining the stiffness of the cantilever [5], the capacitance gradient must be determined ahead of force measurement in electrostatic systems. The roughness of electrode surfaces affects the potential of the capacitor. A large curvature of the electrode surface leads to a small density of charge when a voltage is applied across the electrodes, while a small curvature results in a large charge density. Moreover, the burrs would lead to point discharge and affects dC/dz. For manufacturing the capacitor, the effect of surface roughness on the potential and dC/dz was simulated by Comsol. As shown in Figure 2(a), surface roughness causes a considerable change in the potential of a capacitor, compared to that of a capacitor with a smooth surface. The electric field lines are concentrated on the roughness. The effect of surface roughness on dC/dz for different gaps between the two electrodes ($\delta = 50$ μm, 100 μm, 200 μm, and 300 μm) is shown in Figure 2(b). Obviously, the effect of surface roughness increased with the decrease in δ. For the gap of 300 μm, the relative uncertainty of dC/dz was 0.04% at a surface roughness of 1.1 μm. Therefore, ultraprecision machining was employed for their manufacture. The cylindrical form deviations were below 1 μm. In order to minimize the electric charge accumulation phenomenon caused by the rough surface, the external surface of the inner electrode and the internal surface of the outer electrode were limited to 3 nm. This ensured uniformity in the energy density of the electric field between the electrodes.

3. Newton Interpolation Method

Noise (creep, ground vibration, and airflow) causes limitations in force resolution. The measured force will be drowned by the noise, and therefore, it cannot be measured accurately. Further, the noise will be amplified by the spring. As the inner electrode is fixed on the spring, the position of the inner electrode will vary due to noise. The ABA method can be used to eliminate the linear creep. C_{real} is the real value, $A(X_A, Y_A)$, $B(X_B, Y_B)$, and $C(X_C, Y_C)$ are the measured values, A and B are the values measured without the load, and C is the value with the load. The linear creep can be eliminated by fitting C_{Lf} with $(A + B)/2$. However, the ABA method would be invalid, as the nonlinear noise would lead to a large uncertainty, e_L, as shown in Figure 3.

To eliminate the effect of nonlinear noise, the Newton interpolation method was adopted, as shown in Figure 3. Sample points A_1 and B_1 were added among A and B. In this way, 5 sample points were used to complete a single force measurement. To reduce the effect of higher order noise, more sample points are need. For example, four sample

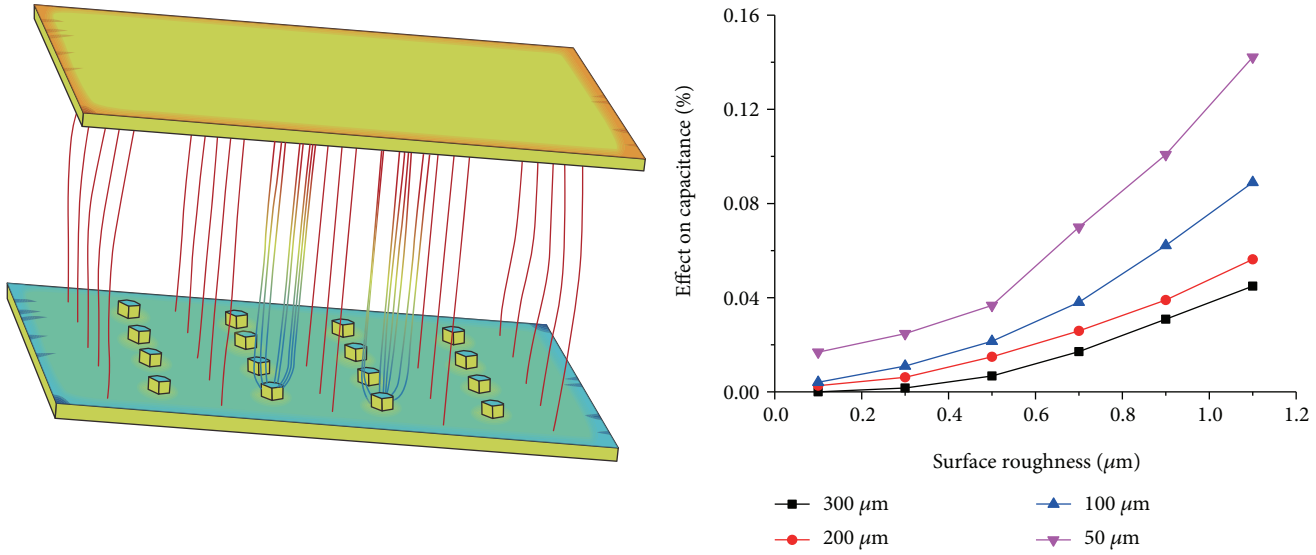

(a) (b)

FIGURE 2: Effect of surface roughness on dC/dz. (a) Simulated potential of the capacitor with surface roughness. (b) Effect of surface roughness on dC/dz at different δ.

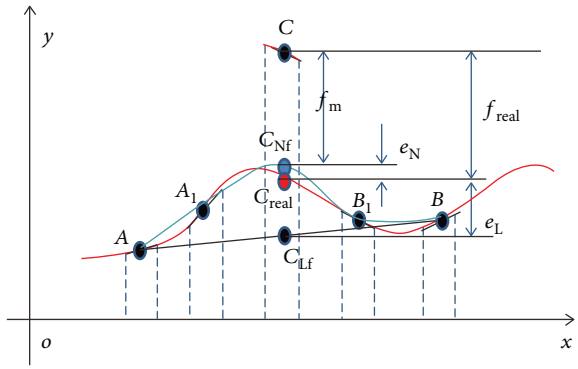

FIGURE 3: Newton interpolation method to reduce the effect of vibration.

points can eliminate the effect of third-order noise; however, higher order noise still affects the results.

The red line indicates real noise, the blue line is the fitting line of the Newton interpolation method, and the black line is the fitting line of the ABA method. $C_{Nf}(x_{Nf}, y_{Nf})$ is the fitting value that uses A, A_1, B, and B_1 with Newton interpolation according to (3):

$$\begin{aligned} C_{NF}(x,y) = {} & y_A + f[x_A, x_{A1}](x - x_A) \\ & + f[x_A, x_{A1}, x_B](x - x_A)(x - x_{A1}) \\ & + f[x_A, x_{A1}, x_B, x_{B1}](x - x_A)(x - x_{A1})(x - x_B), \end{aligned} \tag{3}$$

where $f[x_A, x_{A1}]$, $f[x_A, x_{A1}, x_B]$, and $f[x_A, x_{A1}, x_B, x_{B1}]$ are the Newton interpolations. $f_m = y_c - y_{CNf}$ is the output of the loading force. The deviations of C_{Nf} and C_{real} are small, whereas the deviation of C_{Lf} and C_{real} are very large.

Unlike the "difference method," NIM predicts the value of C_{real} by the approximation of C_{Nf}. Using the values of several known points, an approximation was made in the range of other points.

4. Capacitance Gradient Measurement Results

To measure dC/dz, the outer electrode is fixed on a nanolifting stage with a resolution of 1 nm, which was calibrated using a laser interferometer. Meanwhile, a capacitance bridge (AH2700 with a resolution of 1 aF) is used to measure the capacitance. In this way, the capacitance gradient could be traced in SI units of length and capacitance.

The displacement value of the outer electrode and the capacitance between the electrodes are shown in Figures 4(a) and 4(b). The displacement range was 50 μm and the capacitance range was 0.05 pF. To evaluate the capacitance and displacement, the signals were averaged over a period of 6 s starting from 3 s, when the capacitance was stable.

The capacitance in each step is extracted by NIM, which is shown in Figure 4(c). The points (A1, A2, A3, and A4) are used to predict the value of C_{Nf}. The real value, C_m, is calculated by $C - C_{Nf}$. In this way, the nonlinear noise would be reduced by NIM.

The displacement-capacitance curve was used to calculate dC/dz with straight-line fitting. It has a good linearity with the displacement and capacitance, as shown in Figure 4(d). It is observed that all the capacitances of the upward steps are larger than that of the downward steps. The deviation in capacitance between the upward and downward steps was about 30 fF. The capacitance values were very close in the process of upward and downward movement, and the capacitance gradient was stable. The average capacitance gradient for nine time measurements was found to be 0.93764 pF/mm, and the standard variance was 3.5×10^{-4} pF/mm. The relative standard deviation was 0.004%, which ensures good repeatability. If simply the mean of A1, A2, A3, and A4 is used as the estimated

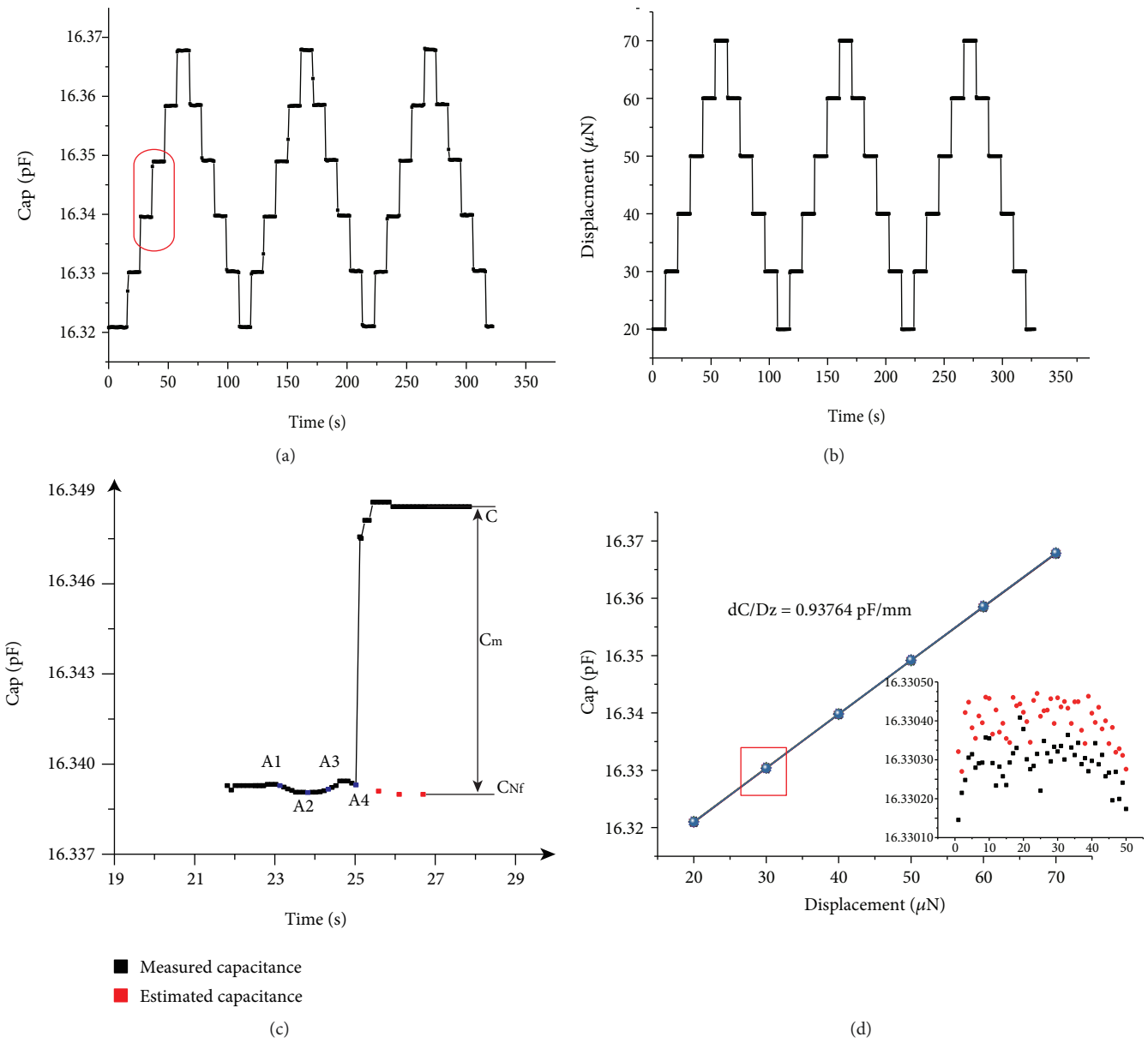

Figure 4: Capacitance gradient measurement results. (a) Capacitance of 3 cycles with 6 steps. (b) Displacement of 3 cycles with 6 steps. (c) Capacitance calculation by NIM. (d) Capacitance-displacement curves for 60 cycles.

capacitance, the relative standard deviation will be much larger, about 0.03%.

5. AFM Cantilever Stiffness Measurement

The stiffness of AFM cantilever [13–15] was measured based on the electrostatic force. The typical value of stiffness ranges from 5.1 to 48 N/m. The cantilever was fixed on a nanolocator having a resolution of 1 nm and a range 100 μm.

The tip of the cantilever was moved to touch the load button tip, as shown in Figure 5(a). Null balance was adopted to measure the loaded force, and a discretized proportional-integral-derivative (PID) controller was used to control the position of the inner electrode. The nanolocator was moved in 2 μm steps from 0 μm to 10 μm. It took about 100 s to complete a single scan. This movement was repeated 10 times over a period of about 1000 s. The displacement and the voltages applied to restore the inner electrode to its initial position are shown in Figures 5(b) and 5(c).

The voltage required to restore the inner electrode to its initial position for each step was extracted by NIM and is shown in Figure 6. The voltage signal includes nonlinear noise and could not be used to calculate the force directly. The points (A1, A2, A3, and A4) were used to predict the value V_{Nf}. The real value, V_{m}, was calculated by $V - V_{\mathrm{Nf}}$. In this way, the nonlinear noise could be reduced by NIM.

The hysteresis is checked by applying electrostatic force. As hysteresis is rather small compared to the uncertainty of the electrostatic force, the uncertainty of hysteresis could be ignored in this experiment. Surface potential is the potential

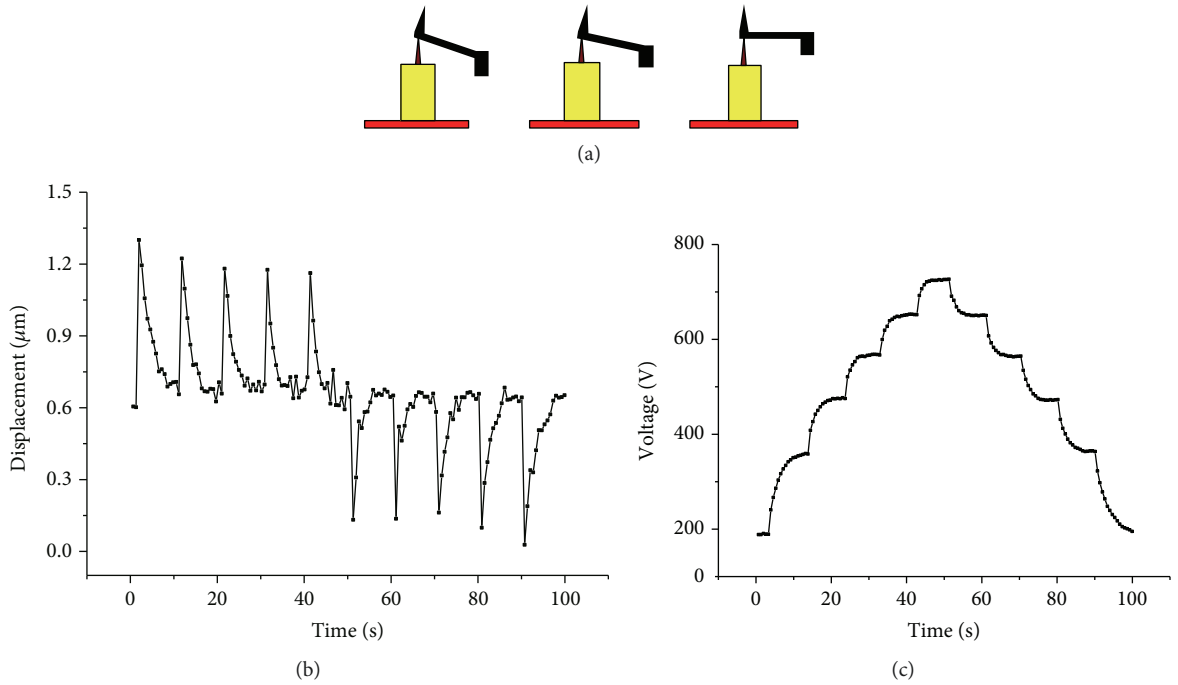

Figure 5: Measurement of cantilever stiffness based on electrostatic force. (a) Measurement sketch. (b) Displacement of spring for 1 cycle. (c) Voltage output to restore the inner electrode to its initial position.

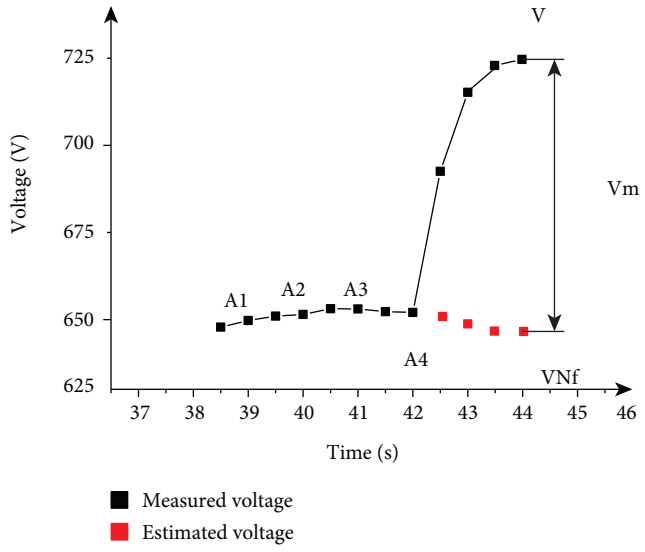

Figure 6: Voltage calculation by NIM.

difference between the electrodes resulting from the hypothesized surface field effects. The relative uncertainty comes from surface potential can be calculated by

$$U_{ur} = \frac{U_s}{2U}, \tag{4}$$

where U_s is surface potential. Though surface potential can be as large as a few tenths of a volt, the uncertainty comes from surface potential is very small, because the voltage U is about hundreds of volts. U_{ur} is less than 0.1% and could be ignored in this paper.

Table 1: Stiffness test results.

Type of cantilever	Nominal value of stiffness (N/m)	Typical value (N/m)	Measured value (N/m)	Standard deviation (N/m)	Relative (%)
NSG01	1.45–15.1	5.1	1.426976	0.00614	0.430
NSG10	3.1–37.6	11.8	15.26733	0.06171	0.404
NSG20	28–91	48	26.46524	0.05269	0.199
TESP	/	42	12.83741	0.07352	0.573

The uncertainty of observation time would lead to the uncertainty of the measurement results. The observation time of displacement is controlled by crystal oscillator with a high precision. The effect of observation time could be ignored. All underlying instruments had been calibrated at China Metrology Institute [10].

The stiffness test results are shown in Table 1. The relative standard deviation is small (less than 0.6%). If simply the mean of A1, A2, A3, and A4 is used, the relative standard deviation will be much larger and could reach up to 2.5%. These results show that our system is very stable and produces repeatable results.

From the results of the capacitance gradient and stiffness calibration for various AFM cantilevers using the system, NIM could reduce the effect of nonlinear low-frequency noise. NIM would be invalid for signals with high-frequency noise, because the high-frequency noise would lead to inaccurate approximation. The system was placed on an isolation platform with a natural vibration of 1 Hz.

Table 2: Uncertainty budget for cantilever calibration.

Type of cantilever	Displacement (%)	Force (%)	Contact position (%)	Repeatability (%)	Relative combined uncertainty (%)
NSG01	0.03	1.3	1.2	0.4	1.8
NSG10	0.03	0.8	1.6	0.4	1.8
NSG20	0.12	0.8	1.7	0.2	1.9
TESP	0.12	0.8	0.7	0.6	1.2

The noise above 1 Hz would be filtered by the isolation platform; therefore, NIM is valid for this system and the results are very stable and repeatable.

6. Discussion

The uncertainties due to many factors such as force, displacement, and position can be estimated from the type B evaluation.

Firstly, the uncertainty of the displacement was evaluated. The displacement was measured by a capacitive feedback sensor that was integrated into the nanostage. The nanostage was calibrated by a laser interferometer. The uncertainty was estimated as 3 nm. For NSG01 and NSG10, the nanolocator was moved from 0 μm to 10 μm in 2 μm steps. For NSG20 and TESP, the nanolocator was moved from 0 μm to 2.5 μm in 0.5 μm steps. The relative uncertainties for the 2.5 μm and 10 μm displacements were conservatively estimated to be 0.12% and 0.03%, respectively.

Secondly, the gravities of 1 mg and 10 mg standard weights were compared using electrostatic force, and the uncertainties of force was established as 1.3% and 0.8%, respectively, according to the uncertainty estimate in [11].

To avoid cantilever tip damage, the back of the cantilever was contacted with a load button, as shown in Figure 5(a). This scheme results in contact position error. To observe the contact position, a microscope (MX20) with an amplification factor of 20 was used to obtain the side view. The microscope was calibrated using a traceable block gauge. It is very important to reduce the effect of distortion, as it will cause a deviation in the length. To reduce the influence of distortion, the cantilever should be placed at the centre of the visual field. Considering the offset of the load-button tip position compared to its apex, we estimated the uncertainty in position as 0.5 μm. The stiffness of the rectangular reference cantilever is inversely proportional to the cube of the length of the cantilever. The lengths of NSG01, NSG10, and NSG20 were 125 μm, 95 μm, and 90 μm, respectively. The uncertainty due to positioning was 1.9%, 1.7%, and 1.4%. For the cantilever TESP, the uncertainty due to positioning was 0.7%, as estimated by finite element analysis (FEM).

The uncertainty sources, force, displacement, and position are independent. The covariance between the uncertainties could be estimated as zero. The stated combined total uncertainty, u, is determined by taking the root sum square of the contributions of individual uncertainty sources to the total uncertainty, as shown in Table 2. Summarizing these rather systematic influences, the combined relative uncertainty was determined to be 2%.

7. Conclusions

In this study, to measure dC/dz and the stiffness calibration of various AFM cantilevers accurately, Newton interpolation method was adopted. The effect of surface roughness on the capacitance gradient was analysed quantitatively. The capacitance gradient was measured accurately with a relative standard deviation of 0.004%, which indicates that this system is very stable. In addition, the AFM cantilever stiffness was measured using this system to evaluate the performance of the system, and the combined relative uncertainty was determined to be 2%. The results of stiffness calibration show that our system is very stable and produces repeatable results. From the results of the capacitance gradient calculation and stiffness calibration of various AFM cantilevers using the system, it can be seen that NIM is a valid and effective method for reducing the effect of nonlinear low-frequency noise, which is difficult to be removed by other methods.

Data Availability

The data used to support the findings of this study are available from the corresponding author upon request.

Conflicts of Interest

The authors declare no conflict of interest.

Acknowledgments

The authors thank the National Natural Science Foundation of China (No. 51805367 and 51175377) and the Tianjin Natural Science Foundation (No. 17JCYBJC19000) for their support.

References

[1] Y. Fujii, "Dynamic force calibration method for force transducers," in *Proceedings of the 21st IEEE Instrumentation and Measurement Technology Conference (IEEE Cat. No.04CH37510)*, pp. 352–357, Como, Italy, 2004.

[2] D. B. Newell, J. A. Kramar, J. R. Pratt, D. T. Smith, and E. R. Williams, "The NIST microforce realization and measurement project," *IEEE Transactions on Instrumentation and Measurement*, vol. 52, no. 2, pp. 508–511, 2003.

[3] R. Leach, D. Chetwynd, L. Blunt et al., "Recent advances in traceable nanoscale dimension and force metrology in the UK," *Measurement Science and Technology*, vol. 17, no. 3, pp. 467–476, 2006.

[4] V. Nesterov, "Facility and methods for the measurement of micro and nano forces in the range below 10^{-5} N with a

resolution of 10^{-12} N (development concept)," *Measurement Science and Technology*, vol. 18, no. 2, pp. 360–366, 2007.

[5] J. R. Pratt and J. A. Kramar, "SI realization of small forces using an electrostatic force balance," in *Proceedings of IMEKO XVIII World Congress*, pp. 1–6, Rio de Janeiro, Brazil, September 2006.

[6] M. S. Kim, J. H. Choi, Y. K. Park, and J. H. Kim, "Atomic force microscope cantilever calibration device for quantified force metrology at micro- or nano-scale regime: the nano force calibrator (NFC)," *Metrologia*, vol. 43, no. 5, pp. 389–395, 2006.

[7] S.-J. Chen and S.-S. Pan, "Nanonewton force generation and detection based on a sensitive torsion pendulum," *IEEE Transactions on Instrumentation and Measurement*, vol. 58, no. 4, pp. 897–901, 2009.

[8] S. J. Chen and S. S. Pan, "A force measurement system based on an electrostatic sensing and actuating technique for calibrating force in a micronewton range with a resolution of nanonewton scale," *Measurement Science and Technology*, vol. 22, no. 4, article 045104, 2011.

[9] Y. Zheng, L. Song, G. Hu et al., "Improving environmental noise suppression for micronewton force sensing based on electrostatic by injecting air damping," *Review of Scientific Instruments*, vol. 85, no. 5, article 055002, 2014.

[10] Y. Zheng, L. Song, G. Hu et al., "The multi-position calibration of the stiffness for atomic-force microscope cantilevers based on vibration," *Measurement Science and Technology*, vol. 26, no. 5, article 055001, 2015.

[11] L. Song, Y. Zheng, G. Hu et al., "Highly sensitive, precise, and traceable measurement of force," *Instrumentation Science & Technology*, vol. 44, no. 4, pp. 386–400, 2016.

[12] Y. S. Ku, "Optimization of axisymmetric parametric model for electrostatic force balance," *Measurement Science and Technology*, vol. 15, no. 10, pp. 2108–2112, 2004.

[13] S. J. Chen, S. S. Pan, Y. S. Yeh, and Y. C. Lin, "Measurement of cantilever spring constant using an electrostatic sensing and actuating force measurement system," *Measurement Science and Technology*, vol. 25, no. 11, article 115006, 2014.

[14] A. Torii, M. Sasaki, K. Hane, and S. Okuma, "A method for determining the spring constant of cantilevers for atomic force microscopy," *Measurement Science and Technology*, vol. 7, no. 2, pp. 179–184, 1996.

[15] D. Georgakaki, S. Mitridis, A. A. Sapalidis, E. Mathioulakis, and H. M. Polatoglou, "Calibration of tapping AFM cantilevers and uncertainty estimation: comparison between different methods," *Measurement*, vol. 46, no. 10, pp. 4274–4281, 2013.

[16] L. Wang and Q. Zhou, "*Nepenthes* pitchers: surface structure, physical property, anti-attachment function and potential application in mechanical controlling plague locust," *Chinese Science Bulletin*, vol. 59, no. 21, pp. 2513–2523, 2014.

[17] L. Wang and Q. Zhou, "Friction force of locust *Locusta migratoria manilensis* (Orthoptera, Locustidae) on slippery zones of pitchers from four *Nepenthes* species," *Tribology Letters*, vol. 44, no. 3, pp. 345–353, 2011.

[18] X. Huang, S. Chen, S. Guo, W. Zhao, and S. J. Jin, "Magnetic charge mad magnetic field distributions in ferromagnetic pipe," *Applied Computational Electromagnetics Society Journal*, vol. 28, no. 8, pp. 737–746, 2013.

[19] H. Wu, F. Zhang, S. Cao, S. Xing, and X. Qu, "Absolute distance measurement by intensity detection using a mode-locked femtosecond pulse laser," *Optics Express*, vol. 22, no. 9, pp. 10380–10397, 2014.

[20] C. L. Dong, C. Q. Yuan, X. Q. Bai, X. P. Yan, and Z. Peng, "Tribological properties of aged nitrile butadiene rubber under dry sliding conditions," *Wear*, vol. 322-323, pp. 226–237, 2015.

[21] C. Dong, C. Yuan, X. Bai, X. Yan, and Z. Peng, "Study on wear behaviour and wear model of nitrile butadiene rubber under water lubricated conditions," *RSC Advances*, vol. 4, no. 36, pp. 19034–19042, 2014.

[22] L. Gao, Y. Liu, T. Ma, R. Shi, Y. Hu, and J. Luo, "Effects of interfacial alignments on the stability of graphene on Ru(0001) substrate," *Applied Physics Letters*, vol. 108, no. 26, article 261601, 2016.

[23] L. Gao, X. Ding, T. Lookman, J. Sun, and E. K. H. Salje, "Metastable phase transformation and hcp-ω transformation pathways in Ti and Zr under high hydrostatic pressures," *Applied Physics Letters*, vol. 109, no. 3, article 031912, 2016.